



Thermodynamic assessments of the Bi–Nd and Bi–Tm systems

C.P. Wang^a, H.L. Zhang^a, A.T. Tang^b, F.S. Pan^b, X.J. Liu^{a,*}

^a Department of Materials Science and Engineering, College of Materials, and Research Center of Materials Design and Applications, Xiamen University, No. 422 Siming South Road, Xiamen 361005, Fujian, PR China

^b College of Materials Science and Engineering, Chongqing University, Chongqing 400045, PR China

ARTICLE INFO

Article history:

Received 6 November 2009

Received in revised form 1 March 2010

Accepted 2 March 2010

Available online 9 March 2010

Keywords:

Phase diagrams

Rare earth alloys and compounds

Thermodynamic modeling

ABSTRACT

By using the calculation of phase diagrams (CALPHAD) method, the thermodynamic assessments of the Bi–Nd and Bi–Tm systems were carried out based on the available experimental data including thermodynamic properties and phase equilibria. Gibbs free energies of the liquid, hcp, bcc, dhcp and rho phases in the Bi–Nd and Bi–Tm systems were modeled by the subregular solution model with the Redlich–Kister formula, and those of the intermetallic compounds (BiNd₂, Bi₃Nd₅, Bi₃Nd₄, BiNd, Bi₂Nd, BiTm and Bi₃Tm₅ compounds) in these two binary systems were described by the two-sublattice model. An agreement between the present calculated results and experimental data was obtained.

© 2010 Elsevier B.V. All rights reserved.

1. Introduction

Rare earth (RE) elements are added into the Mn–Bi system to form the RE₃MnBi₅ and RE₂Mn₃Bi₆ ternary compounds with good electrical and magnetic properties [1]. Moreover, RE elements are important for Bi-based superconductors with great technological interest. At the same time, the interest in these compounds of bismuthides of RE elements has increased after the discovery of high-temperature superconductivity [2]. Therefore, it is important to understand the phase equilibria in the Bi–RE binary system.

The CALPHAD method, which is a powerful tool to cut down on cost and time during development of materials [3], effectively provides a clear guideline for materials design. In order to design high-performance alloys with rare earth elements, it is important to develop a thermodynamic database including rare earth elements alloys. Currently, our group is focusing on the development of a thermodynamic database of rare earth alloy system [4–12], which is important for the design of alloys with additions of rare earth elements. As a part of this thermodynamic database, this work is to present the thermodynamic descriptions of the Bi–Nd and Bi–Tm binary systems based on the available experimental data by means of the CALPHAD method.

2. Thermodynamic model

The information of stable solid phases including prototype, strukturbericht designation, modeling phase and used models in the Bi–Nd [13] and Bi–Tm [14] systems is listed in Table 1.

2.1. Solution phases

Gibbs free energies of the liquid, hcp, bcc, dhcp and rho phases in the Bi–Me (Me: Nd or Tm) system were modeled by the subregular solution model with the Redlich–Kister formula [15]. The molar Gibbs free energies of solution phases in the Bi–Me system are given as follows:

$$G_m^\phi = \sum_{i=\text{Bi,Me}} {}^0G_i^\phi x_i + RT \sum_{i=\text{Bi,Me}} x_i \ln x_i + x_{\text{Bi}}x_{\text{Me}} \sum_{m=0}^n {}^mL_{\text{Bi,Me}}^\phi (x_{\text{Bi}} - x_{\text{Me}})^m, \quad (1)$$

where ${}^0G_i^\phi$ is the Gibbs free energy of pure component i taken from SGTE database [16]; x_i represents the mole fraction of the component i ; R is the gas constant and T is the absolute temperature; ${}^mL_{\text{Bi,Me}}^\phi$ is the binary interaction parameter and is expressed as:

$${}^mL_{\text{Bi,Me}}^\phi = a_m + b_m T, \quad (2)$$

where the values of a_m and b_m are evaluated in the present work based on the experimental data.

* Corresponding author. Tel.: +86 592 2187888; fax: +86 592 2187966.
E-mail address: lxj@xmu.edu.cn (X.J. Liu).

Table 1
The stable solid phases and the used models in the Bi–Nd [13] and Bi–Tm [14] systems.

System	Phase	Prototype	Strukturbericht designation	Modeling phase	Used models
Bi–Nd	(Bi)	α As	A7	(Bi, Nd)	SSM
	Bi_2Nd	Distorted anti- La_2Sb	...	$(\text{Bi})_2(\text{Nd})_1$	SM
	BiNd	NaCl	B1	$(\text{Bi})_1(\text{Nd})_1$	SM
	Bi_3Nd_4	anti- Th_3P_4	...	$(\text{Bi})_3(\text{Nd})_4$	SM
	Bi_3Nd_5	Mn_5Si_3	D8 ₈	$(\text{Bi})_3(\text{Nd})_5$	SM
	BiNd_2	La_2Sb	...	$(\text{Bi})_1(\text{Nd})_2$	SM
	αNd	αLa	A3'	(Bi, Nd)	SSM
	βNd	W	A2	(Bi, Nd)	SSM
	Bi–Tm	(Bi)	α As	A7	(Bi, Tm)
BiTm		NaCl	B1	$(\text{Bi})_1(\text{Tm})_1$	SM
Bi_3Tm_5		Bi_3Y_5	...	$(\text{Bi})_3(\text{Tm})_5$	SM
(Tm)		Mg	A3	(Bi, Tm)	SSM

Note: SSM: subregular solution model and SM: sublattice model.

2.2. Intermetallic compounds

The intermetallic compounds of the BiNd_2 , Bi_3Nd_5 , Bi_3Nd_4 , BiNd and Bi_2Nd in the Bi–Nd binary system, and the BiTm and Bi_3Tm_5 in the Bi–Tm binary system are treated as stoichiometric compounds. The Gibbs free energy of the Bi_pMe_q compound can be expressed by the two-sublattice model [17], which is formulated as:

$$\Delta G_f^{\text{Bi}_p\text{Me}_q} = G_m^{\text{Bi}_p\text{Me}_q} - p^0 G_{\text{Bi}}^{\text{ref}} - q^0 G_{\text{Me}}^{\text{ref}} = a' + b'T, \quad (3)$$

where the $\Delta G_f^{\text{Bi}_p\text{Me}_q}$ represents the Gibbs free energy of formation per mole of formula unit Bi_pMe_q . The values of a' and b' are evaluated in the present work.

3. Experimental information

3.1. Bi–Nd system

Gschneidner and Calderwood [13] studied the phase diagram in the Bi–Nd system, where there exist three solution phases ((Bi), αNd and βNd) and five intermetallic compounds (BiNd_2 , Bi_3Nd_5 , Bi_3Nd_4 , BiNd and Bi_2Nd). Abulkhaev [18] reported the phase diagram in the Bi–Nd system using differential thermal analysis, X-ray powder diffraction, and metallography. There are two eutectic reactions of the $\text{L} \leftrightarrow (\text{Bi}) + \text{Bi}_2\text{Nd}$ at $269 \pm 2^\circ\text{C}$ and $\text{L} \leftrightarrow \text{BiNd}_2 + \beta\text{Nd}$ at $950 \pm 10^\circ\text{C}$, and a eutectoid reaction of the $\beta\text{Nd} \leftrightarrow \alpha\text{Nd} + \text{BiNd}_2$ at $835 \pm 10^\circ\text{C}$, and four peritectic reactions of the $\text{L} + \text{BiNd} \leftrightarrow \text{Bi}_2\text{Nd}$ at $660 \pm 5^\circ\text{C}$, $\text{L} + \text{Bi}_3\text{Nd}_5 \leftrightarrow \text{BiNd}_2$ at $1260 \pm 15^\circ\text{C}$, $\text{L} + \text{Bi}_3\text{Nd}_4 \leftrightarrow \text{Bi}_3\text{Nd}_5$ at $1450 \pm 15^\circ\text{C}$, and $\text{L} + \text{BiNd} \leftrightarrow \text{Bi}_3\text{Nd}_4$ at $1565 \pm 15^\circ\text{C}$. The phase diagram of the Bi–Nd system reviewed by Okamoto [19] is shown in Fig. 1.

In addition, there are three reports on the experimental data of thermodynamic properties. Viksman and Gordienko [20] determined the enthalpy of formation of the BiNd phase at 25°C with respect to the rho (Bi) and dhcp (Nd) phases, Borsese et

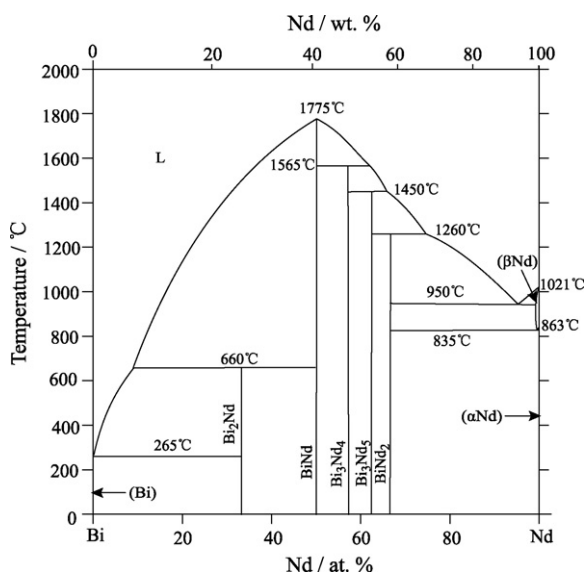


Fig. 1. The phase diagram of the Bi–Nd system reviewed by Okamoto [19].

Table 2
Thermodynamic parameters in the Bi–Nd and Bi–Tm systems.

System	Parameters in each phase (J/mol)
Bi–Nd	Liquid phase, formula (Bi, Nd)
	${}^0L_{\text{Bi,Nd}}^{\text{liq}} = -240,000 - 10T$
	${}^1L_{\text{Bi,Nd}}^{\text{liq}} = 26,500$
	${}^2L_{\text{Bi,Nd}}^{\text{liq}} = 30,000 + 22T$
	${}^3L_{\text{Bi,Nd}}^{\text{liq}} = -20,000$
	Bcc phase, formula (Bi, Nd)
	${}^0L_{\text{Bi,Nd}}^{\text{bcc}} = -150,000$
	${}^1L_{\text{Bi,Nd}}^{\text{bcc}} = 50,000$
	Dhcp phase, formula (Bi, Nd)
	$G_{\text{Bi}}^{\text{dhcp}} = G_{\text{Bi}}^{\text{rho}} + 5000$
	${}^0L_{\text{Bi,Nd}}^{\text{dhcp}} = 100,000$
	Rhombohedral phase, formula (Bi, Nd)
	$G_{\text{Nd}}^{\text{rho}} = G_{\text{Nd}}^{\text{dhcp}} + 5000$
	${}^0L_{\text{Bi,Nd}}^{\text{rho}} = 50,000$
	BiNd_2 phase, formula $(\text{Bi})_{0.333}(\text{Nd})_{0.667}$
	$\Delta G_f^{\text{BiNd}_2} = -107,107 + 19.2T$
Bi_3Nd_5 phase, formula $(\text{Bi})_{0.375}(\text{Nd})_{0.625}$	
$\Delta G_f^{\text{Bi}_3\text{Nd}_5} = -108814.2 + 14.9T$	
Bi_3Nd_4 phase, formula $(\text{Bi})_{0.429}(\text{Nd})_{0.571}$	
$\Delta G_f^{\text{Bi}_3\text{Nd}_4} = -110,690 + 11.4T$	
BiNd phase, formula $(\text{Bi})_{0.5}(\text{Nd})_{0.5}$	
$\Delta G_f^{\text{BiNd}} = -110,000 + 7T$	
Bi_2Nd phase, formula $(\text{Bi})_{0.667}(\text{Nd})_{0.333}$	
$\Delta G_f^{\text{Bi}_2\text{Nd}} = -81,200 + 9.83T$	
Bi–Tm	Liquid phase, formula (Bi, Tm)
	${}^0L_{\text{Bi,Tm}}^{\text{liq}} = -210,000$
	${}^1L_{\text{Bi,Tm}}^{\text{liq}} = -15,000$
	${}^2L_{\text{Bi,Tm}}^{\text{liq}} = 38,300 + 8T$
	Hcp phase, formula (Bi, Tm)
	${}^0L_{\text{Bi,Tm}}^{\text{hcp}} = -121,500$
	Rhombohedral phase, formula (Bi, Tm)
	$G_{\text{Tm}}^{\text{rho}} = G_{\text{Tm}}^{\text{hcp}} + 5000$
	${}^0L_{\text{Bi,Tm}}^{\text{rho}} = 1000$
	BiTm phase, formula $(\text{Bi})_{0.5}(\text{Tm})_{0.5}$
	$\Delta G_f^{\text{BiTm}} = -99,000 + 9.3T$
Bi_3Tm_5 phase, formula $(\text{Bi})_{0.375}(\text{Tm})_{0.625}$	
$\Delta G_f^{\text{Bi}_3\text{Tm}_5} = -73,565 + 4.35T$	

al. [21] measured the enthalpies of formation of the Bi_3Nd_5 , Bi_3Nd_4 , BiNd and Bi_2Nd phases at 27 °C with respect to the rho (Bi) and dhcp (Nd) phases, and Kober et al. [22] reported the enthalpy and entropy of formation of the Bi_2Nd phase between 537 and 746 °C with different reference states.

3.2. Bi–Tm system

Abdusalyamova et al. [23] determined the phase diagram in the Bi–Tm system by means of differential thermal analysis and X-ray diffraction, and determined the existence of the Bi_3Tm_5 and BiTm intermetallic compounds in the Bi–Tm system. In this system, there are two eutectic reactions of the $L \leftrightarrow (\text{Bi}) + \text{BiTm}$ at 266 °C and $L \leftrightarrow (\text{Tm}) + \text{Bi}_3\text{Tm}_5$ at 1140 °C, and a peritectic reaction of the $L + \text{BiTm} \leftrightarrow \text{Bi}_3\text{Tm}_5$ at 1510 °C, and the compound BiTm melts at 1780 °C, and the bismuth solubility in thulium is about 1 at.%. The Bi–Tm phase diagram reviewed by Okamoto [24] is shown in Fig. 2. However, more recently Abulkhaev [25] have studied the Bi–Tm phase diagram by means of differential thermal analysis, X-ray diffraction and microstructural analysis, and reported there are two eutectic reactions of the $L \leftrightarrow (\text{Bi}) + \text{BiTm}$ at 268 ± 5 °C and $L \leftrightarrow (\text{Tm}) + \text{Bi}_3\text{Tm}_5$ at 1137 ± 10 °C, and a peritectic reaction of the $L + \text{BiTm} \leftrightarrow \text{Bi}_3\text{Tm}_5$ at 1417 ± 15 °C, and the compound BiTm melts at 1737 ± 20 °C, and neglected the solubility of (Bi) in (Tm). The thulium metal have higher purity in Ref. [25] than Ref. [23], and the heating rate (30 °C min^{-1}) in Ref. [23] is faster than that (5 °C min^{-1}) in Ref. [25]. Thus, the invariant reactions reported by Abulkhaev [25] are more reasonable, we give more weight to the data of invariant reactions from Ref. [25] during our assessment.

No experimental thermodynamic data for the Bi–Tm system were reported. The experimental enthalpies of formation of monobismuthides are about from -120 to -90 kJ/mol of atoms in the Bi–RE system reported by Abdusalyamova et al. [23].

4. Results and discussion

The optimization was carried out using the PARROT module in the Thermo-Calc program developed by Sundman et al. [26]. The phase diagram and thermochemical data were used as input to the program. Each piece of selected information was given a certain weight by personal judgment, and verified by trial and error during the assessment, until most of the selected experimental information was reproduced within the expected uncertainty limits. All the evaluated parameters of each phase in the Bi–Nd and Bi–Tm systems are listed in Table 2.

4.1. Bi–Nd system

Fig. 3 shows the calculated Bi–Nd phase diagram compared with experimental data [18,19]. The calculated phase diagram is in good agreement with the experimental data. The calculated invariant reactions in the Bi–Nd system are listed in Table 3.

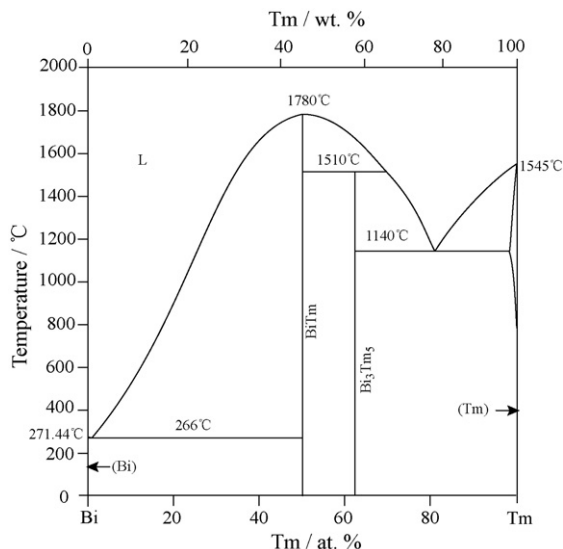


Fig. 2. The phase diagram of the Bi–Tm system reviewed by Okamoto [24].

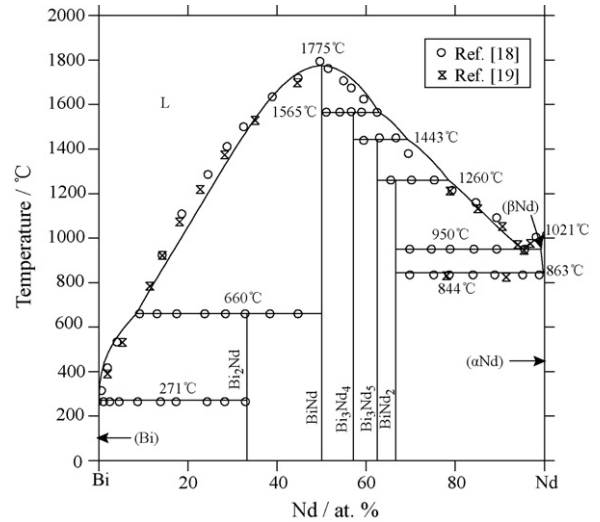


Fig. 3. Calculated phase diagram in the Bi–Nd system compared with experimental data [18,19].

As shown in Fig. 4, the calculated enthalpies of formation of intermetallic phases at 27 °C with respect to rho (Bi) and dhcp (Nd) phases are compared with the experimental data [20,21]. The calculated enthalpies of formation of intermetallic phases with respect to the rho (Bi) and dhcp (Nd) phases using solid line and with respect to the liquid (Bi) and dhcp (Nd) phases using dashed line at 627 °C are shown in Fig. 5 together with the experimental data [22]. In addition, the calculated entropies of formation of intermetallic phases with respect to the rho (Bi) and dhcp (Nd) phases using solid line and with respect to the liquid (Bi) and dhcp (Nd) phases using dashed line at 627 °C are illustrated in Fig. 6 together with the experimental data [22]. It is seen that the calculated enthalpies of formation of the Bi_3Nd_5 phase and BiNd_2 phase are more negative than those obtained by Borsese et al. [21], as shown in Fig. 4. By considering the agreements of the most of the experimental data including the data of phase equilibria and thermodynamic properties, we think that this calculated result can be accepted.

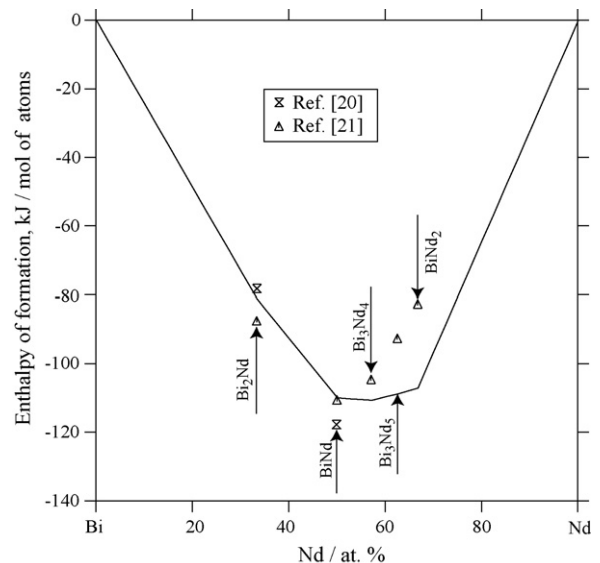


Fig. 4. Calculated enthalpies of formation of intermetallic phases at 27 °C compared with experimental data [20,21] in the Bi–Nd system.

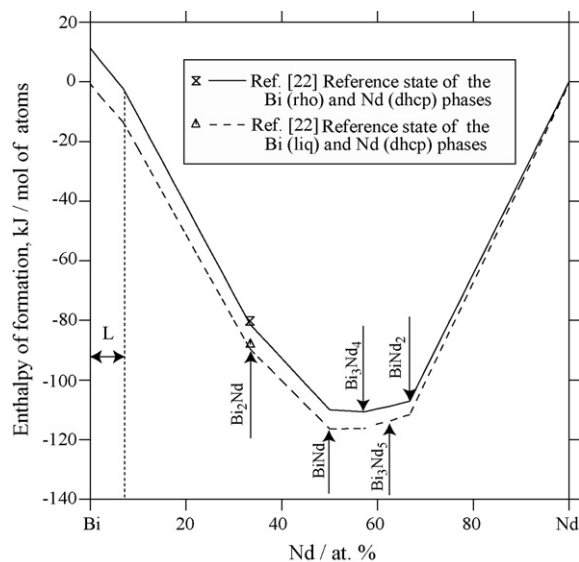


Fig. 5. Calculated enthalpies of formation of intermetallic phases at 627 °C compared with experimental data [22] in the Bi–Nd system.

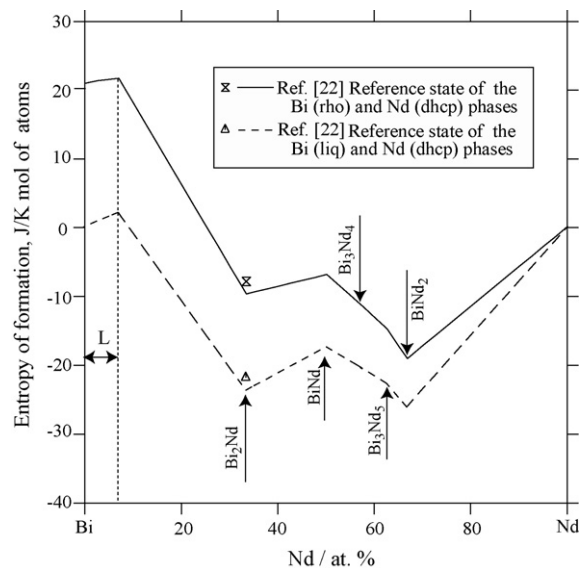


Fig. 6. Calculated enthalpies of formation of intermetallic phases at 627 °C compared with experimental data [22] in the Bi–Nd system.

Table 3
Invariant reactions in the Bi–Nd system.

Reaction	Reaction type	Composition (Nd/at.%)			T (°C)	Reference
$L \leftrightarrow (Bi) + Bi_2Nd$	Eutectic	–	0	33.3	269 ± 5	[18]
		–	0	33.3	265	[19]
		0.4	0	33.3	271	This work
$L + BiNd \leftrightarrow Bi_2Nd$	Peritectic	–	50	33.3	660 ± 5	[18]
		8.4	50	33.3	660	This work
$(\beta Nd) \leftrightarrow (\alpha Nd) + BiNd_2$	Eutectoid	–	100	66.7	835 ± 10	[18]
		99.9	100	66.7	844	This work
$L \leftrightarrow BiNd_2 + (\beta Nd)$	Eutectic	–	66.7	–	950 ± 10	[18]
		95.1	66.7	99.1	950	This work
$L + Bi_3Nd_5 \leftrightarrow BiNd_2$	Peritectic	–	62.5	66.7	1260 ± 15	[18]
		78.5	62.5	66.7	1260	This work
$L + Bi_3Nd_4 \leftrightarrow Bi_3Nd_5$	Peritectic	–	57.1	62.5	1450 ± 15	[18]
		69.3	57.1	62.5	1443	This work
$L + BiNd \leftrightarrow Bi_3Nd_4$	Peritectic	–	50	57.1	1565 ± 15	[18]
		62.9	50	57.1	1565	This work
$L \leftrightarrow BiNd$	Congruent	–	50	–	1775 ± 20	[18]
		–	50	–	1775	This work

Table 4
Invariant reactions in the Bi–Tm system.

Reaction	Reaction type	Composition (Tm/at.%)			T (°C)	Reference
$L \leftrightarrow (Bi) + BiTm$	Eutectic	–	0	50	268 ± 5	[25]
		–	0	50	266	[23]
		2.1	0	50	266	This work
$L \leftrightarrow (Tm) + Bi_3Tm_5$	Eutectic	–	–	62.5	1137 ± 10	[25]
		~81.0	~99.0	62.5	1140	[23]
		82.5	99.0	62.5	1137	This work
$L + BiTm \leftrightarrow Bi_3Tm_5$	Peritectic	–	50	62.5	1417 ± 15	[25]
		–	50	62.5	1510	[23]
		69.5	50	62.5	1414	This work
$L \leftrightarrow BiTm$	Congruent	–	50	–	1737 ± 20	[25]
		–	50	–	1780	[23]
		–	50	–	1740	This work

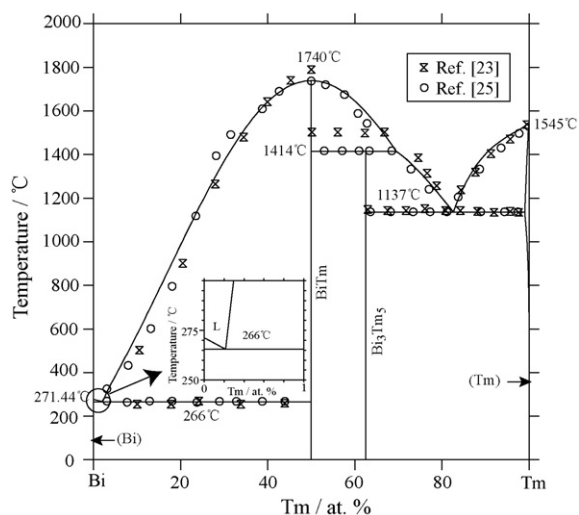


Fig. 7. Calculated phase diagram of the Bi–Tm system compared with experimental data [23,25].

4.2. Bi–Tm system

Comparison of the calculated Bi–Tm phase diagram with experimental data [23,25] is shown in Fig. 7, where the calculated phase diagram of invariant reactions is in good agreement with the phase diagram reviewed by Abulkhaev [25]. The calculated invariant reactions in the Bi–Tm system are listed in Table 4, where a good agreement between the calculated and experimental temperatures for these invariant reactions has been obtained.

Fig. 8 shows the calculated enthalpies of formation of intermetallic phases at 27 °C with respect to rho (Bi) and hcp (Tm) phases in the Bi–Tm system. The summary of enthalpies of formation of monobismuthides including our calculated result in the Bi–RE system is shown in Fig. 9. The present calculated enthalpy of formation of the BiTm phase is -99 kJ/mol of atoms, which is in the range of -120 to -90 kJ/mol of atoms reported by Abdusalyamova et al. [23]. Thus, the calculated enthalpies of formation of the BiTm phase are reasonable. Although the calculated enthalpies of formation of intermetallic phases in the Bi–Tm system need to be experimentally determined in the future. These predicted results give an

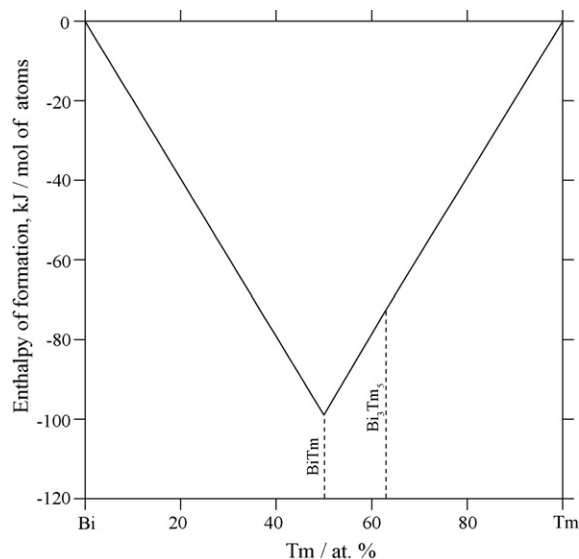


Fig. 8. Calculated enthalpies of formation of intermetallic phases at 27 °C with respect to rho (Bi) and hcp (Tm) phases in the Bi–Tm system.

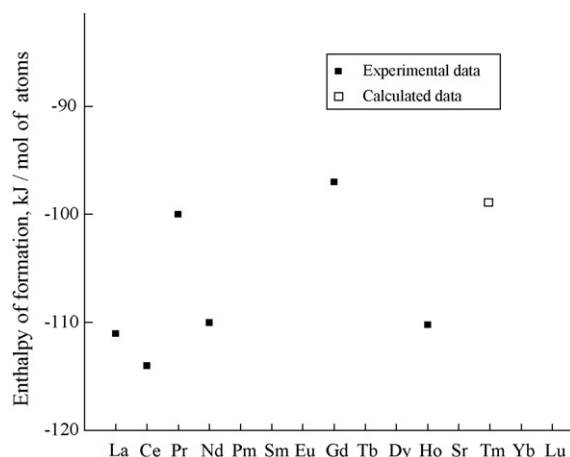


Fig. 9. Enthalpies of formation of monobismuthides in the Bi–RE system.

useful information for determination of enthalpies of formation of intermetallic phases by experiments.

5. Conclusions

The phase diagrams in the Bi–Nd and Bi–Tm binary systems were thermodynamically assessed by considering the experimental data including phase equilibria and thermodynamic data. A consistent set of thermodynamic parameters has been optimized and most of the experimental information can be satisfactorily reproduced on the basis of the optimized thermodynamic parameters.

Acknowledgements

This work was supported by the National Natural Science Foundation of China (No. 50725413), the Ministry of Education, PR China (No. 707037), the National Basic Research Program of China (No. 2007CB613704), the Ministry of Science and Technology, PR China (No. 2009AA03Z101), and Fujian Province and Xiamen City Departments of Science and Technology (Nos. 2009I0024 and 3502Z20093001).

References

- [1] O.Y. Zelinska, A. Mar, *Inorg. Chem.* 47 (2008) 297–305.
- [2] P.E. Fazin, D.D. Zaitsev, Yu.D. Tret'yakov, M. Jansen, *Inorg. Mater.* 37 (2001) 960–964.
- [3] L. Kaufman, H. Bernstein, *Computer Calculation of Phase Diagram*, Academic Press, New York, 1970.
- [4] S.L. Wang, C.P. Wang, X.J. Liu, K. Ishida, *J. Alloys Compd.* 476 (2009) 245–252.
- [5] S.L. Wang, C.P. Wang, X.J. Liu, K. Ishida, *J. Alloys Compd.* 476 (2009) 187–192.
- [6] C.P. Wang, X. Chen, X.J. Liu, F.S. Pan, K. Ishida, *J. Alloys Compd.* 458 (2008) 166–173.
- [7] X.J. Liu, X. Chen, C.P. Wang, *J. Alloys Compd.* 468 (2009) 116–121.
- [8] C.P. Wang, J. Wang, X.J. Liu, I. Ohnuma, R. Kainuma, K. Ishida, *J. Alloys Compd.* 453 (2008) 174–179.
- [9] C.P. Wang, Z. Lin, X.J. Liu, *J. Alloys Compd.* 469 (2009) 123–128.
- [10] C.P. Wang, A.Q. Zheng, X.J. Liu, K. Ishida, *J. Alloys Compd.* 478 (2009) 197–201.
- [11] C.P. Wang, S.H. Guo, A.T. Tang, F.S. Pan, X.J. Liu, K. Ishida, *J. Alloys Compd.* 482 (2009) 67–72.
- [12] C.P. Wang, H.L. Zhang, S.L. Wang, Z. Lin, X.J. Liu, A.T. Tang, F.S. Pan, *J. Alloys Compd.* 481 (2009) 291–295.
- [13] K.A. Gschneidner Jr., F.W. Calderwood, *Bull. Alloy Phase Diag.* 10 (4a) (1989) 444.
- [14] K.A. Gschneidner Jr., F.W. Calderwood, *Bull. Alloy Phase Diag.* 10 (4a) (1989) 454.
- [15] O. Redlich, A.T. Kister, *Ind. Eng. Chem.* 40 (1948) 345–348.
- [16] A.T. Dinsdale, *CALPHAD* 15 (1991) 317–425.
- [17] M. Hillert, L.I. Stafansson, *Acta Chem. Scand.* 24 (1970) 3618.
- [18] V.D. Abulkhaev, *J. Inorg. Chem.* 46 (4) (2001) 580–583.
- [19] H. Okamoto, *J. Phase Equilib.* 23 (2) (2002) 191.

- [20] G.S. Viksman, S.P. Gordienko, Poroshk. Metall. 7 (1987) 63.
- [21] A. Borsese, R. Capelli, S. Delfino, R. Ferro, Thermochim. Acta 8 (1974) 393.
- [22] V.I. Kober, V.A. Dubinin, I.F. Nichkov, S.R. Kanevskii, Zh. Fiz. khim. 60 (1986) 197.
- [23] M.N. Abdusalyamova, A.G. Chuiko, E.I. Shishkin, O.I. Rachmatov, J. Alloy. Compd. 240 (1996) 272–277.
- [24] H. Okamoto, J. Phase Equilib. 20 (2) (1999) 164.
- [25] V.D. Abulkhaev, Inorg. Mater. 39 (1) (2003) 47–49.
- [26] B. Sundman, B. Jansson, J.O. Andersson, CALPHAD 9 (1985) 153–190.